P H Y S I C A L   R E V I E W   L E T T E R S

Tunable Spin Gaps in a Quantum-Confined Geometry

Emmanouil Frantzeskakis,[1] Stéphane Pons,[1,2,*] Hossein Mirhosseini,[3] Jürgen Henk,[3] Christian R. Ast,[4] and Marco Grioni[1]

[1]*Laboratoire de Spectroscopie Électronique, Institut de Physique des Nanostructures,*
École Polytechnique Fédérale de Lausanne (EPFL), station 3, CH-1015 Lausanne-Switzerland
[2]*Laboratoire de Physique des Matériaux, Nancy-Université, CNRS, Boulevard des Aiguillettes,*
B.P. 239, F-54506 Vandoeuvre lès Nancy, France
[3]*Max-Planck-Institut für Mikrostrukturphysik, Weinberg 2, D-06120 Halle (Saale), Germany*
[4]*Max-Planck-Institut für Festkörperforschung, D-70569 Stuttgart, Germany*
(Received 26 May 2008; published 7 November 2008)

We have studied the interplay of a giant spin-orbit splitting and of quantum confinement in artificial Bi-Ag-Si trilayer structures. Angle-resolved photoelectron spectroscopy reveals the formation of a complex spin-dependent gap structure, which can be tuned by varying the thickness of the Ag buffer layer. This provides a means to tailor the electronic structure at the Fermi energy, with potential applications for silicon-compatible spintronic devices.

In nonmagnetic centrosymmetric bulk solids like silicon, electronic states of opposite spin have the same energy. A surface or an interface breaks the translational invariance of a three-dimensional crystal. Thus, as predicted by Bychkov and Rashba [1], the spin-orbit (SO) interaction can lead to spin-split electronic states in two-dimensional electron gases (2DEG), in asymmetric quantum wells [2], at a surface or at an interface [3,4]. The size of the splitting is related to the strength of the atomic SO coupling (i.e., to the gradient of the atomic potential [5]) and to the potential gradient perpendicular to the confinement [6]. An unexpectedly large splitting was recently reported for a Bi-Ag surface alloy grown on a Ag(111) single crystal [7]. It is attributed to an additional in-plane gradient of the surface potential, hence being a direct consequence of the chemical alloy configuration [7,8].

The spin-orbit interaction could be used to control via a gate voltage the dynamics of spins injected into a semiconductor [2,9–11]. Moreover, the spin Hall effect—also induced by the SO interaction—could find applications in new spintronic devices [12,13] which rely neither on magnetic materials nor on optical pumping. Interfaces between silicon and materials exhibiting large spin-orbit splitting are therefore expected to open novel vista for spintronics. The challenge is to control the electronic states and spin polarization at the Fermi level which determine the electron and spin transport through interfaces [14,15] and nanostructures. Among the heavy metals which exhibit strong spin-orbit interactions, bismuth may be favored for environmental considerations. Experiments on thin layers of bismuth on silicon have evidenced a SO splitting in the Bi surface states, but not of their bulk counterparts [16,17]. Moreover, it was observed that the splitting is removed by the hybridization between surface and bulk states.

In this Letter we explore a different approach. We fabricated trilayer systems composed of a Bi-Ag surface alloy [7], a thin Ag buffer layer of variable thickness d, and a Si

(111) substrate [Fig. 1(a)]. Along the z direction, the vacuum/BiAg/Ag/Si related potential is asymmetric and SO splitting of delocalized electronic states is expected. The good interfacial adhesion of the silver film makes the system stable at room temperature (RT) and results in a sharp interface. We investigated the complex interface by angle-resolved photoelectron spectroscopy (ARPES), supported by first-principles electronic-structure calculations. We find that the SO splitting is large. We also find that, due
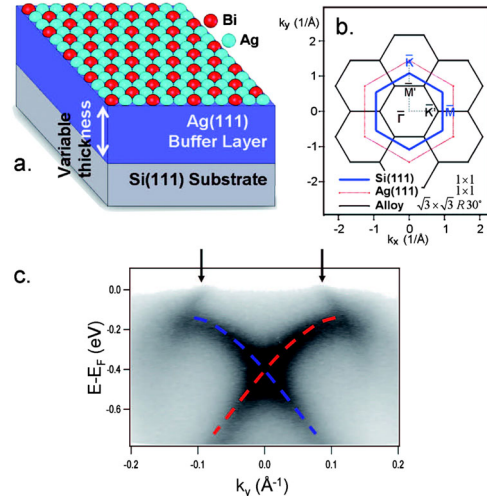

FIG. 1 (color online). (a) Schematic view of a trilayer sample. The $\sqrt{3} \times \sqrt{3}R30°$ Bi-Ag alloy is grown on a Ag buffer—whose thickness can be varied—deposited on a silicon substrate. (b) First Brillouin zones of the surface structures. The symmetry lines $\bar{\Gamma}\bar{K}\bar{M}$ and $\bar{\Gamma}\bar{K}'\bar{M}'$ refer to Si(111) and to the alloy, respectively. (c) ARPES intensity of the surface states of a Bi-Ag alloy grown on a thick Ag layer deposited on Si(111) along $\bar{\Gamma}\bar{K}'\bar{M}'$. This system is similar to the alloy grown on a Ag(111) single crystal. Dashed lines indicate the branches of opposite spins of the sp_z surface state. Arrows point out bands of p_xp_y symmetry. Close to $\bar{\Gamma}$ all bands exhibit a rotational symmetry around the surface normal.

to quantum confinement in the buffer layer, the electronic structure exhibits patches of highly spin-polarized spectral density. The spin-dependent density of states close to the Fermi energy can be tuned by the thickness of the Ag buffer.

The experiments were performed with a multichamber setup under an ultrahigh vacuum. During preparation, Si(111) (highly phosphorus doped, resistivity 0.009–0.011 $\Omega \cdot$ cm) was flashed at 1200 °C by direct current injection. After the flashes, the substrate was cooled slowly in order to obtain a sharp 7×7 signature in low-energy electron diffraction (LEED). The Ag films were deposited with a homemade Knudsen cell while the sample was kept at 80 K and then annealed at 400 K. The quality of the silver thin film was checked by LEED. Ag grows in the [111] direction [18]. The $\sqrt{3} \times \sqrt{3}R30°$ Bi-Ag surface alloy was obtained by depositing 1/3 ML of Bi with an EFM3 Omicron source on the sample at RT followed by a soft annealing. Angle-resolved photoemission spectroscopy (ARPES) spectra were acquired at RT and 55 K with a PHOIBOS 150 Specs analyzer. We used a monochromatized and partially polarized GammaData VUV 5000 high brightness source of 21.2 eV photons.

The first-principles electronic-structure calculations are based on the local spin-density approximation to density functional theory, as implemented in relativistic multiple-scattering theory (Korringa-Kohn-Rostoker and layer-Korringa-Kohn-Rostoker methods; for details, see Refs. [7,19]). Spin-orbit coupling is taken into account by solving the Dirac equation. The computer codes used consider the boundary conditions present in experiment, that is the semi-infinite substrate, a buffer of finite thickness, the surface, and the semi-infinite vacuum. The potentials of all sites (atoms) are computed self-consistently, except for the Si substrate which is mimicked by spherical repulsive potentials of 1 Hartree height. This so-called hard-sphere substrate follows the face-centered cubic structure of the Ag buffer. The electronic structure is addressed in terms of the spectral density which is obtained from the imaginary part of the Green function of the entire system. The latter can be resolved with respect to wave vector, site, spin, and angular momentum, thus allowing a detailed analysis of the local electronic structure.

The surface electronic properties of the alloy grown on top of a thick Ag film ($d = 80$ monolayers (ML)), as obtained by ARPES [Fig. 1(c)], agree with those of the alloy grown on a Ag(111) single crystal [7]. The spin-split bands which belong to electronic states with sp_z character cross at $\bar{\Gamma}$ (in-plane wave vector $\mathbf{k}_{\parallel} = 0$). They are well described by parabolas (effective mass $m^* = -0.35m_e$) which are offset by $\Delta k = \pm 0.13$ Å^{-1}. This shift in wave vector is a signature of the aforementioned Rashba effect. Two sets of side bands stem from electronic states of mainly $p_x p_y$ character which are also spin polarized but less split [7,8,20]. The $p_x p_y$ bands cross the Fermi level at $k_F^{\text{inner}} \approx \pm 0.09$ Å^{-1} and $k_F^{\text{outer}} \approx \pm 0.21$ Å^{-1}. Electronic-

structure calculations [7] show that the Bi-Ag surface states are much more strongly localized in the top layer than the Ag(111) or Au(111) Shockley surface states. Thus, the spin-split bands and the giant SO splitting are not directly affected by the Ag/Si interface for Ag film thickness larger than a few monolayers. This implies that prior results for BiAg/Ag(111) [7] can be transferred to silicon technology [i.e., to BiAg/Ag/Si(111)] at RT.

A new and interesting situation arises for thinner Ag buffer layers, where d is of the order of the attenuation length of the electronic states. The Ag sp states are confined to the Ag film by the potential barrier (image-potential barrier) on the vacuum side (surface) and by the fundamental band gap of Si on the substrate side. This confinement leads to quantized wave vectors along z and to discrete energy levels [21]. These so-called quantum well states (QWS's) play a central role in transport properties [22] and in the coupling of magnetic layers in superlattices [23–25]. Ag/Si(111) QWS's, in particular, have been extensively studied by ARPES [18,26,27]. For Ag(111) films, their in-plane dispersion consists of a set of parabolic bands centered at $\bar{\Gamma}$, with energies determined by the film thickness [Fig. 2(a); $d = 17$ ML]. The electronic fringe structure with a negative parabolic dispersion appears due to the accumulation of QWS's near the k-dependent valence band edge of Si. This is an indirect manifestation of the heavily doped n-type character of the Si(111) substrates used here [18]. The narrow line shapes of the energy
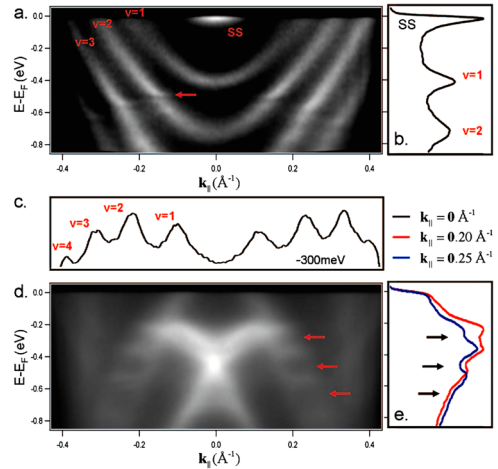

FIG. 2 (color online).   (a) Raw ARPES data along $\bar{\Gamma}\bar{K}$ at 55 K. QWS's in a 17 ML bare Ag buffer deposited on Si(111). These parabolic states are numbered $\nu = 1 \ldots n$. Kinks in the dispersion (arrow) are due to the hybridization of the QWS with the p bands of silicon. SS stands for the Shockley surface state of Ag (111). (b) EDC extracted from Fig. 2(a) at $\bar{\Gamma}$, i.e., $k = 0.0$ Å^{-1}. The 1st and 2nd QWS signatures and the SS are indicated. (c) MDC extracted from Fig. 2(a) at -300 meV shows the successive branches of the QWS. (d) Raw ARPES intensity along $\bar{\Gamma}\bar{M}'$ at 55 K of the Bi-Ag alloy grown on 17 ML of Ag. (e) EDC extracted from Fig. 2(d) for $k = 0.20$ Å^{-1} and $k = 0.25$ Å^{-1}. Arrows indicate gaps of 100–200 meV in the dispersion of the $p_x p_y$ bands.

distribution curves [EDC's; Fig. 2(b)] and momentum distribution curves [MDC's; Fig. 2(c)], and the observation of the electronic fringes reflect the uniformity of the Ag buffers and the high resolution of the experiment.

We now consider the interaction of the spin-split alloy surface states and the QWS's in a BiAg/Ag/Si trilayer, focusing first on a 17 ML thick Ag buffer [Fig. 2(d); i.e., the sample of Fig. 2(a) covered by the Bi-Ag alloy). The Ag Shockley surface state disappears and the resulting surface electronic structure agrees in general with that of the system without Si substrate [BiAg/Ag(111); no QWS's] but shows intensity modulations in both the sp_z and $p_x p_y$ bands. The energy distribution curves, extracted from the raw data, clearly evidence band gaps [Fig. 2(e)].

The remaining signature of the Ag QWS's (at large k values) and the gaps in Bi-Ag surface states are clearly seen even at RT in the second derivative of the ARPES intensities ($d^2 I(E, \mathbf{k}_\parallel)/dE^2$) for samples with selected Ag film thicknesses ($d = 19$, 16, and 10 ML) in Fig. 3. The parabolic in plane dispersion of the QWS's (circles in Fig. 3) is obtained from MDC's of Ag/Si(111) with the corresponding Ag thicknesses [as presented in Fig. 2(c)]. Agreement between the parabolic fits (uncovered Ag buffer) and the QWS's of the alloyed sample is obtained after shifting rigidly the parabolas by 50–150 meV to lower binding energies. These shifts can be attributed to the different reflection properties of the bare Ag surface and

of the Bi-Ag surface alloy [28]. However, the effective masses of the QWS's may also change. Therefore, these fits are to be considered as guides to the eye. Band gaps are found at the intersection of the QWS parabola with both branches of the surface-alloy bands regardless of their symmetry or spin, providing strong evidence of their hybridization. The hybridization is spin selective [29,30]; thus, we can consider in a first approximation that the QWS are spin-degenerate or their spin-splitting is small. For thinner Ag buffers [10 ML; Fig. 3(c)], the number of QWS's is reduced. As a result, the number of band gaps is also decreased but their widths are larger, in particular, for the $p_x p_y$ states.

To further corroborate the above interpretation of the band gaps, first-principles electronic-structure calculations for BiAg/Ag(111) reported in [7,19] were extended. Since the Ag/Si(111) interface is incommensurate [18], we are forced to approximate the Si substrate. Therefore, the confinement of the Ag QWS's by the Si(111) substrate is mimicked by replacing Ag bulk layers by repulsive potentials. The latter provide the complete reflection of the Ag states at the Ag/Si(111) interface. Note that by this means details of the Ag/Si interface are roughly approximated and the binding energies of the theoretical quantum well states may differ from experiment. However, the essential features are well captured, as will be clear from the agreement of experiment and theory discussed below. The systems investigated comprise the Bi-Ag surface alloy, Ag layers, and the substrate built from hard spheres [HS; i.e. BiAg/Ag$_{d-1}$/HS(111)]. The theoretical analysis focuses on the wave vector and spin-resolved spectral density $N(E, \mathbf{k}_\parallel; \sigma)$ at a Bi site ($\sigma = \uparrow$ or $\downarrow$ is the spin quantum number). Spin dependent band gaps are visualized by displaying $\Delta N(E, \mathbf{k}_\parallel) = N(E, \mathbf{k}_\parallel; \uparrow) - N(E, \mathbf{k}_\parallel; \downarrow)$.

For BiAg/Ag(111), the Bi surface states hybridize with Ag bulk states, resulting in a rather blurred spectral density [Fig. 4(a); compare Fig. 1(c) for the experiment]. For the systems with Si substrate, focusing here on exemplary results for $d = 10$ [Fig. 4(b)] and 19 [Fig. 4(c)], quantum well states show up as parabolas centered at $\bar{\Gamma}$. The most striking difference to BiAg/Ag(111) are, however, spin-dependent band gaps at $(E, \mathbf{k}_\parallel)$ points at which the QWS's would cross the Bi bands. With increasing thickness of the Ag buffer, the number of gaps (or QWS's) increases and the width of the gaps decreases. The spectral densities of the Bi states are slightly less blurred than for BiAg/Ag(111) because hybridization with Ag states occurs only at the band gaps, due to quantization. Eventually, we find a shift of the QWS's energies upon covering the Ag buffer with the Bi-Ag alloy, as observed by the experiment.

We now focus on the agreement of the experimental findings and the present theoretical approach. Apart from the similar trends concerning the number and the width of the gaps with varying the buffer layer thickness, theory predicts the experimentally observed strong spectral weight of the remaining ungapped parts of the alloy states.
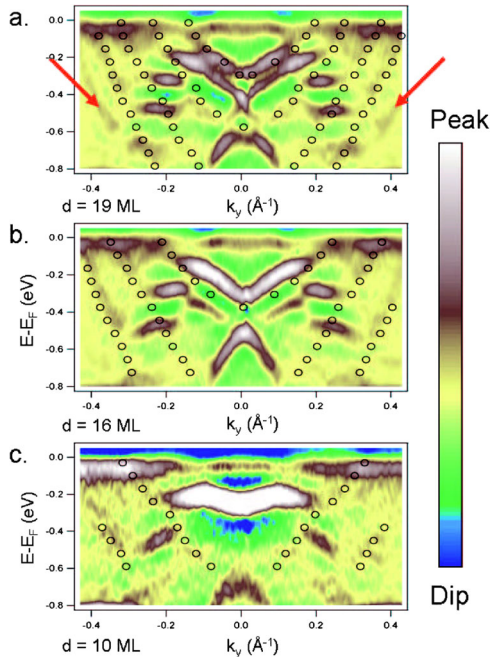

FIG. 3 (color online). (a),(b), and (c) second derivative of the ARPES intensity along $\bar{\Gamma}\bar{M}'$ for three alloy-covered samples at RT with different Ag film thicknesses, respectively, 19, 16, and 10 ML. Circles correspond to MDC fits of the QWS observed on the bare Ag thin films of the corresponding thicknesses shifted by 50–150 meV upwards in order to match the remaining parts of the QWS at large k values after Bi deposition (e.g., red arrows).
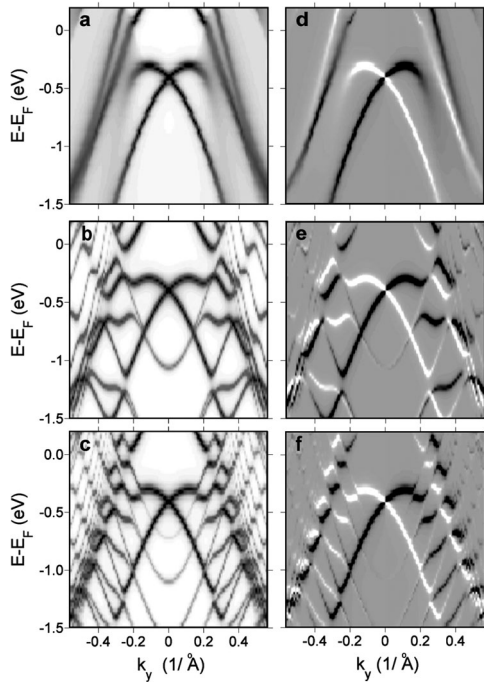
FIG. 4.   Effect of QWS's on the spin-split electronic structure of the Bi/Ag surface alloy, as obtained from first-principles electronic-structure calculations. (a)–(c): The spectral density at the Bi site is displayed as gray scale (with white indicating vanishing spectral weight) for BiAg/Ag(111) (a) and BiAg/Ag/Si(111) for Ag buffer thicknesses $d = 10$ (b) and $d = 19$ (c). The wave vector is chosen as in the experiment (Fig. 3). (d)–(f): The spin polarization of the electronic states is visualized by $\Delta N(E, \mathbf{k}_\parallel)$, i.e., the difference of the spin-up and the spin-down spectral density. White and black indicate positive and negative values, respectively, where gray is for zero ΔN.

Moreover, it points towards the association of the un-gapped parts of the sidebands both with the $p_x p_y$ bands and the continuation of the $s p_z$ band at large wave vectors. The finite experimental resolution prevents us from identifying each single contribution. Nevertheless, both in the experimental (Fig. 3) and the theoretical data [Figs. 4(e) and 4(f)], the overall shape of each ungapped structure of the sidebands exhibits a continuously changing curvature from positive to negative with decreasing d.

By contrast with what has been observed in Bi thin layers on silicon [16,17], the theoretical results of Figs. 4(e) and 4(f) clearly show that the Ag quantum well states are spin-polarized due to the Rashba effect. Close to $\bar{\Gamma}$, the branches of opposite spins of the QWS follow a parabolic dispersion and their momentum separation decreases with the Ag thickness. This feature is evident in the figures which show the spin polarization of the electron states. We now address, in particular, the electronic structure at the Fermi level. For $d = 10$ ML [Fig. 4(e)], highly spin-polarized states show up at $k_\parallel = k_F = 0.22$ Å^{-1}, with a spin polarization of about 33%. On the contrary, a complete gap appears for $d = 19$ ML [Fig. 4(f)]. These findings imply that the spin-dependent electronic structure at

the Fermi level—and thus the transport properties—can be drastically modified by the Ag film thickness.

Our findings for BiAg/Ag/Si(111) trilayers suggest that it is indeed possible to match systems with large spin-orbit splitting [here: BiAg/Ag(111)] with a semiconductor substrate. Furthermore, interfacial properties can be custom tailored, in the present case by a single parameter, namely, the Ag buffer layer thickness. In this respect, multilayer systems which comprise semiconducting Si layers and Rashba-split subsystems (like BiAg/Ag) may be very useful in the development of new spintronics devices. Tuning the band-gap structure at the Fermi level could also be achieved by chemical means, as was demonstrated for $Bi_x Pb_{1-x} Ag_2$ mixed alloys grown on Ag(111) [19]. Peculiar transport properties and spin Hall effects can be anticipated based on this interface, namely, in nanostructured systems or (Bi-Ag-Si) superlattices.

*Electronic address: stephane.pons@epfl.ch
[1] Y. A. Bychkov and E. I. Rashba, JETP Lett. **39**, 78 (1984).
[2] T. Koga et al., Phys. Rev. Lett. **88**, 126601 (2002).
[3] S. LaShell, B. McDougall, and E. Jensen, Phys. Rev. Lett. **77**, 3419 (1996).
[4] E. Rotenberg, J. W. Chung, and S. Kevan, Phys. Rev. Lett. **82**, 4066 (1999).
[5] D. Malterre et al., New J. Phys. **9**, 391 (2007).
[6] F. Forster, S. Hüfner, and F. Reinert, J. Phys. Chem. B **108**, 14692 (2004).
[7] C. R. Ast et al., Phys. Rev. Lett. **98**, 186807 (2007).
[8] J. Premper et al., Phys. Rev. B **76**, 073310 (2007).
[9] S. Datta and B. Das, Appl. Phys. Lett. **56**, 665 (1990).
[10] D. Awshalom and M. Flaté, Nature Phys. **3**, 153 (2007).
[11] J. Nitta et al., Phys. Rev. Lett. **78**, 1335 (1997).
[12] Y. Kato et al., Nature (London) **427**, 50 (2004).
[13] S. Valenzuela and M. Tinkham, Nature (London) **442**, 176 (2006).
[14] F. Greullet et al., Phys. Rev. Lett. **99**, 187202 (2007).
[15] E. Tsymbal et al., Prog. Mater. Sci. **52**, 401 (2007).
[16] T. Hirahara et al., Phys. Rev. Lett. **97**, 146803 (2006).
[17] T. Hirahara et al., Phys. Rev. B **76**, 153305 (2007).
[18] N. Speer, S. Tan, and T.-C. Chiang, Science **314**, 804 (2006).
[19] C. R. Ast et al., Phys. Rev. B **77**, 081407(R) (2008).
[20] F. Meier et al., Phys. Rev. B **77**, 165431 (2008).
[21] T.-C. Chiang, Surf. Sci. Rep. **39**, 181 (2000).
[22] M. Jalochowski et al., Phys. Rev. B **45**, 13 607 (1992).
[23] J. E. Ortega and F. J. Himpsel, Phys. Rev. Lett. **69**, 844 (1992).
[24] J. Ortega et al., Phys. Rev. B **47**, 1540 (1993).
[25] P. Bruno, Phys. Rev. B **52**, 411 (1995).
[26] A. L. Wachs et al., Phys. Rev. B **33**, 1460 (1986).
[27] J. F. Sanchez-Royo et al., Phys. Rev. B **66**, 035401 (2002).
[28] T. Hirahara et al., Phys. Rev. B **78**, 035408 (2008).
[29] C. Didiot et al., Phys. Rev. B **74**, 081404(R) (2006).
[30] I. Barke et al., Phys. Rev. Lett. **97**, 226405 (2006).